DEVELOPMENTAL DYNAMICS 245:678–691, 2016
DOI: 10.1002/DVDY.24409

RESEARCH ARTICLE

Intracellular Golgi Complex Organization Reveals Tissue Specific Polarity During Zebrafish Embryogenesis

Diane S. Sepich* and Lila Solnica-Krezel*

Department of Developmental Biology, Washington University School of Medicine, St Louis, Missouri

Background: Cell polarity is essential for directed migration of mesenchymal cells and morphogenesis of epithelial tissues. Studies in cultured cells indicate that a condensed Golgi Complex (GC) is essential for directed protein trafficking to establish cell polarity underlying directed cell migration. Dynamic changes of the GC intracellular organization during early vertebrate development remain to be investigated. **Results:** We used antibody labeling and fusion proteins in vivo to study the organization and intracellular placement of the GC during early zebrafish embryogenesis. We found that the GC was dispersed into several puncta containing cis- and trans-Golgi Complex proteins, presumably ministacks, until the end of the gastrula period. By early segmentation stages, the GC condensed in cells of the notochord, adaxial mesoderm, and neural plate, and its intracellular position became markedly polarized away from borders between these tissues. **Conclusions:** We find that GC is dispersed in early zebrafish cells, even when cells are engaged in massive gastrulation movements. The GC accumulates into patches in a stage and cell-type specific manner, and becomes polarized away from borders between the embryonic tissues. With respect to tissue borders, intracellular GC polarity in notochord is independent of mature apical/basal polarity, Wnt/PCP, or signals from adaxial mesoderm. *Developmental Dynamics 245:678–691, 2016.* © 2016 Wiley Periodicals, Inc.

Key words: GM130; Tbx16; Wnt/PCP; dispersed; chordamesoderm

Submitted 22 September 2015; First Decision 15 March 2016; Accepted 29 March 2016; Published online 4 April 2016

Introduction

Morphogenetic processes, such as gastrulation, neurulation and organogenesis, involve recurring transitions between epithelial and mesenchymal cellular architecture and dynamic changes of cellular polarity (Lim and Thiery, 2012; Nakaya and Sheng, 2013; Nieto, 2013; Singh and Solecki, 2015). Epithelial cells differ from mesenchymal cells in extent of interactions with cell neighbors, morphology, and intracellular organization (Hay, 2005; Nelson, 2009). Epithelia are composed of tightly adherent cells with well defined apical/basal polarity. This is accomplished through vectorial transport of proteins to apical and basal compartments, which permits different functions at each surface. Protein transport in epithelia often employs apicobasally oriented acentrosomal microtubules (MTs) (Rodriguez-Boulan and Macara, 2014).

Epithelia use a variety of cellular mechanisms to shape tissues. Rearrangement of cells, powered by remodeling of apical cell-cell junctions and basal protrusion, drives epithelial morphogenesis during germ band extension in *Drosophila* and gastrulation in mouse embryos (Blankenship et al., 2006; Zallen, 2007; Levayer and Lecuit, 2013; Williams et al., 2014). Constriction of the apical cell surface drives epithelial bending during vertebrate neurulation or *Drosophila* gastrulation (Nagele et al., 1987; Haigo et al., 2003; Martin et al., 2009; Takeichi, 2014). Further, cells may leave the epithelium to migrate as small clusters or as individual mesenchymal cells (Revenu and Gilmour, 2009; Godde et al., 2010; Nakaya and Sheng, 2013). This entails an epithelial to mesenchymal transition (EMT), where adhesion between cells decreases, allowing cell dispersal and increased motility, and where apical/basal cell polarity is replaced by a leading/trailing edge (or front/rear) polarity (Nelson, 2009; Rodriguez-Boulan and Macara, 2014). MTs in migrating mesenchymal cells are typically arranged radially around the centrosome, which often is positioned between the leading edge and the nucleus (Luxton and Gundersen, 2011; Etienne-Manneville, 2013; Rodriguez-Boulan and Macara, 2014).

For tissue-level functions to emerge, cells must coordinate behaviors and structures with their neighbors. Planar cell polarity coordinates asymmetric cell structures or behaviors across an epithelium or over a mesenchymal cell population (Fanto and McNeill, 2004; Hale and Strutt, 2015). Wnt/planar cell polarity (Wnt/PCP) signaling provides one mechanism for coordinating planar polarity across developing epithelia in the invertebrate *Drosophila* and over epithelial and mesenchymal tissues in vertebrates (Goodrich and Strutt, 2011; Gray et al., 2011; Devenport, 2014). During vertebrate embryogenesis, Wnt/PCP signaling

Grant sponsor: National Institutes of Health/National Institute of General Medical Sciences; Grant number: GM55101.
*Correspondence to: Diane S. Sepich and Lila Solnica-Krezel, Department of Developmental Biology, Washington University School of Medicine in St. Louis, St Louis, MO 63110. Email: sepichd@wustl.edu; solnical@wustl.edu.

Article is online at: http://onlinelibrary.wiley.com/doi/10.1002/dvdy.24409/abstract

controls convergence and extension (C&E) gastrulation movements, neural cell migrations, cilium and cochlear hair cell orientation, nap of fur, and morphogenesis of cardiac, renal, and neural organs (Montcouquiol et al., 2006; Gray et al., 2011; Wallingford, 2012; Devenport, 2014). Wnt/PCP-dependent asymmetries extend to intracellular organization, including microtubule and actin cytoskeletons (Sepich et al., 2011; Vladar et al., 2012; Mahaffey et al., 2013) and actin-based protrusions in *Drosophila* and vertebrates, (Song et al., 2010; Wallingford, 2010); Wnt/PCP signaling also regulates localized activity of F-actin and myosin II during C&E and neurulation (Marlow et al., 2002; Kinoshita et al., 2008; Shindo and Wallingford, 2014; Newman-Smith et al., 2015; Ossipova et al., 2015). We previously reported that Wnt/PCP signaling posteriorly biased the location of the centrosome in mesenchymal cells engaged in C&E gastrulation movements in zebrafish (Sepich et al., 2011). There is evidence that the microtubule cytoskeleton is not only regulated downstream of Wnt/PCP, but that it can also be used to establish planar cell polarity. First, Wnt/PCP components Frizzled-GFP and Dishevelled-GFP were found to move along apical asymmetric MTs in *Drosophila* imaginal disc epithelia (Shimada et al., 2006; Matis et al., 2014). Second, in vertebrates, the Wnt/PCP core molecule Vangl2 engages a specific transport mechanism from the trans-Golgi network to reach the proximal cell surface (Guo et al., 2013). Hence, functional interactions between Wnt/PCP signaling and the GC could underlie cell polarity and morphogenesis.

The GC has an important role in directed migration of cultured cells by establishing cell polarity through polarized protein trafficking and directed secretion (Yadav and Linstedt, 2011; Rodriguez-Boulan and Macara, 2014; Sanders and Kaverina, 2015). The GC is an organelle that modifies newly made proteins, builds lipids, and sorts them to various cellular compartments. Proteins move from cis- to trans-Golgi cisternae, then transit to their final cellular compartments. The typical form of the GC is a compact ribbon structure composed of stacked Golgi lumens or cisternae joined laterally by tubular membranes (Thyberg and Moskalewski, 1999; Sutterlin and Colanzi, 2010; Rios, 2014). The GC is often tightly associated with the centrosome and the nucleus. Condensed GC architecture and asymmetrical position within the cell are believed to be needed for directed cell migration and polarized protein trafficking in a variety of cultured cells, including mouse embryonic fibroblasts (Drabek et al., 2006), HeLa cells (Yadav et al., 2009), and human retinal pigmented epithelial cells (Hurtado et al., 2011; Vinogradova et al., 2012). A polarized GC position may enhance polarized protein trafficking further by acting as a second MT organizing center that nucleates MTs asymmetrically to the nearby leading edge of a motile cell (Efimov et al., 2007). Loss of GC-nucleated MTs impairs polarized protein trafficking and directed migration (Efimov et al., 2007; Miller et al., 2009). Whether GC architecture or Golgi-nucleated MTs play a similar role in the gastrulating vertebrate embryos is not known.

Here we asked what GC architecture was present in migrating cells in the gastrulating zebrafish embryo, and if GC architecture or its intracellular distribution were dependent on Wnt/PCP signaling. To address these questions, we analyzed distribution of GC components in living or fixed zebrafish embryos engaged in gastrulation or early somitogenesis. We report that, rather than appearing as a single compact ribbon, the GC was dispersed into numerous small stacked cisternae (ministacks) in most embryonic cells from cleavage stages until the end of the gastrula period. The GC condensed into a ribbon in the differentiating superficial epithelial periderm (enveloping layer, or EVL) by mid-gastrulation stage, and in the notochord and adaxial mesoderm by early segmentation stages. We also found that, by early segmentation, the intracellular position of the GC became markedly polarized away from tissue borders in transient embryonic structures, including the notochord, adaxial mesoderm, and neural plate. Our experiments indicate that this intracellular polarization of the GC is independent of well developed apical/basal polarity, Wnt/PCP signaling, or signals originating from the adaxial mesoderm. Our observations, from cleavage through gastrulation stages in a vertebrate embryo, imply that the GC can function while in a dispersed condition. The condensed GC ministacks became intracellularly polarized with respect to tissue borders, revealing Wnt/PCP-independent polarity cues in dorsal tissues.

Results

Golgi Complex is Fragmented in Early Zebrafish Embryo

During zebrafish gastrulation, cells undergoing C&E movements show coordinated planar polarity that depends on Wnt/PCP signaling: Cells elongate and align mediolaterally to migrate as a cohesive group or intercalate in a polarized fashion (Jessen et al., 2002; Yin et al., 2008). Additionally during C&E, Wnt/PCP signaling biases the intracellular position of the centrosome to reside posteriorly in dorsolateral ectoderm and mesoderm (Sepich et al., 2011). As the Golgi ribbon accumulates around the centrosome in many types of cells (Thyberg and Moskalewski, 1999), we wondered if the GC was polarized in a similar fashion during gastrulation cell movements in the zebrafish embryo.

To visualize the intracellular organization and distribution of the GC in cells of gastrulating zebrafish embryos, we employed whole-mount immunofluorescence using a monoclonal antibody against endogenous GM130, a cis-Golgi resident protein (Nakamura et al., 1995). At mid-gastrulation (80% epiboly, 8 hours post fertilization [hpf]), confocal microscopy revealed GM130 labeling as multiple puncta in each cell, instead of a single Golgi ribbon (Fig. 1A–F). GM130 puncta were detected on the periphery of the nucleus and throughout the cytosol (Fig. 1F). We observed a dispersed GC distribution in both ectodermal and mesodermal cells (Fig. 1A,B,D,E), both having mesenchymal character at this stage of development. In contrast, in the most superficial epithelium of the gastrula, the EVL (Kimmel et al., 1995), we observed a more compact GC surrounding the nucleus starting variably at mid-gastrulation and remaining apparent at segmentation stages (Fig. 1C,I,S).

During mitosis in cultured cells, the single GC breaks up and disperses through the cytoplasm, with the GC ribbon separating laterally into ministacks and then into vesicles (Thyberg and Moskalewski, 1999; Rabouille and Kondylis, 2007; Mironov and Beznoussenko, 2011) that accumulate at the spindle poles and are partitioned into daughter cells. With the close of mitosis, Golgi vesicles travel along MTs toward the centrosome, where they rebuild the ribbon (Yadav and Linstedt, 2011). Most cells in zebrafish embryos that were analyzed here (gastrulation to segmentation stages, 6–13 hpf) are passing through cell cycles 13–16 and reach cell cycle 18 by 24 hpf (Kane and Kimmel, 1993; Kimmel et al., 1994; Kane, 1999). Cell divisions are no longer synchronous at these stages across the embryo, although sister

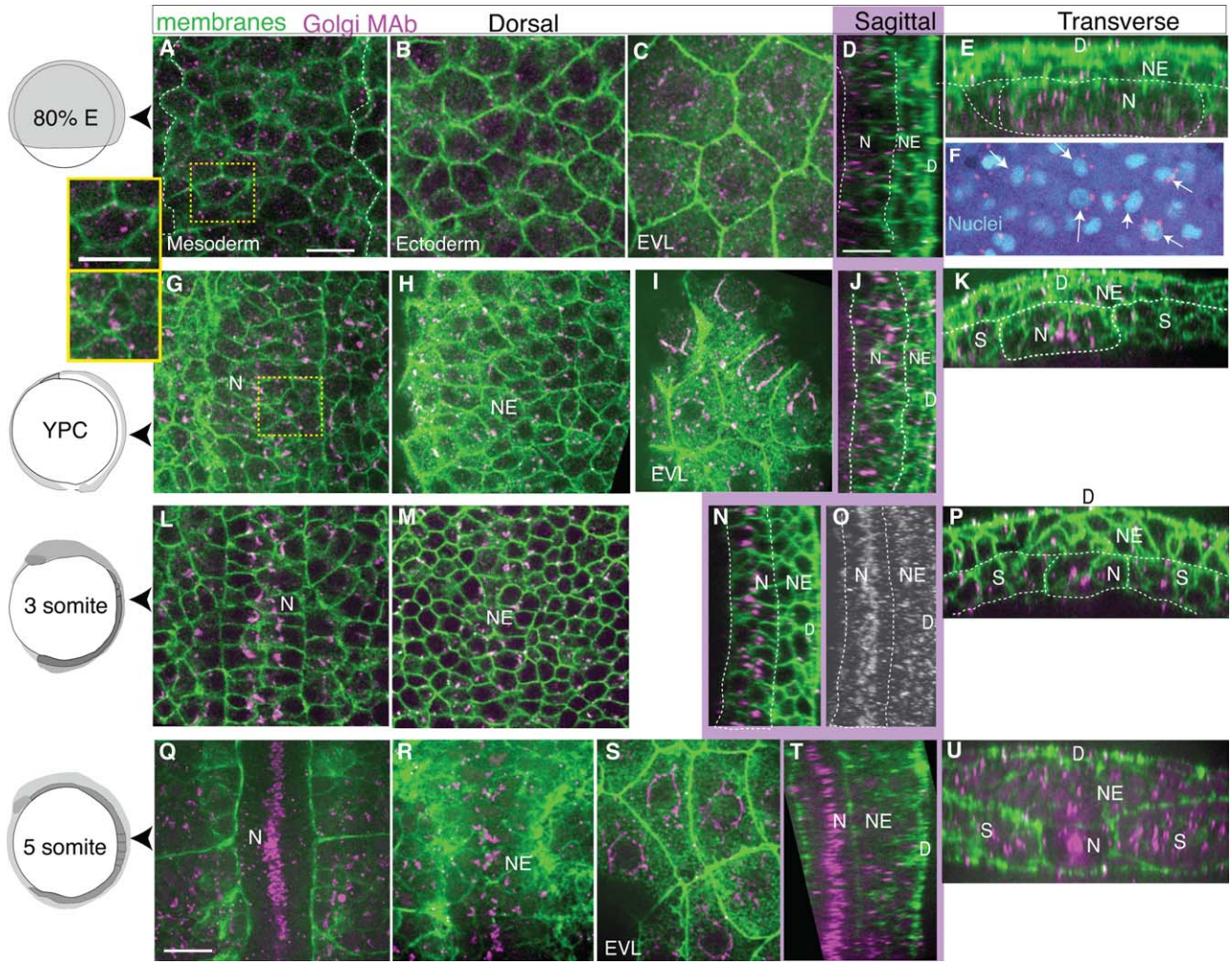

Fig. 1. Dynamic intracellular organization and position of the Golgi Complex monitored by monoclonal antibody labeling of endogenous GM130 protein, a cis-Golgi compartment protein. GM130 in magenta, cell membranes in green. Left column: age of embryos. **A–F**: Mid-gastrulation embryo (80% epiboly, 8.3 hpf). A: Dorsal mesoderm, inset: one cell. B: Neurectoderm. C: Enveloping layer. D: Notochord in sagittal view. E: Transverse view, line on notochord, adaxial mesoderm, neurectoderm. F: Arrows indicate nuclei with perinuclear GC, nuclei in cyan. **G–K**: Late gastrulation–stage embryo (YPC, 9.5 hpf). G: Notochord, inset: one cell. H: Neural plate. I: EVL. J: Sagittal view of notochord, neural plate, line on notochord. K: Transverse view, line at notochord, adaxial mesoderm, and neural plate. **L–P**: 3 somite stage embryo (11 hpf). L: Notochord and somites. M: Neural plate. N: Sagittal view of notochord and neural plate. O: Z-projected sagittal view of the GC in notochord. P: Transverse view, notochord, somites, neural plate. **Q–U**: 5 somite stage embryo (11.7 hpf). Q: Notochord and somites. R: Ventral neural plate. S: EVL. T: Sagittal view of notochord and neural plate. U: Transverse view, notochord, somites, and neural plate. D, dorsal; N, notochord; NE, neurectoderm; S, somites or paraxial mesoderm. Scale bars = 20 μm.

cells may divide at the same time (Kane and Kimmel, 1993; Mendieta-Serrano et al., 2013). Accordingly, we observed a few dividing cells during time-lapse recording (data not shown). In the forming daughter cells, GC puncta gathered in two clusters (presumably around centrosomes), indicating the ability to travel on mitotic MTs (data not shown). However, most cells that we observed with dispersed GC were in interphase. EVL cells are either mitotically arrested or in very long cell cycles at this time (Kane, 1999; Mendieta-Serrano et al., 2013). Several nascent cell types are reported to undergo their final cell division at mid-gastrulation (cell cycle 15), including primary neurons and some axial midline cells (Kane, 1999). When notochord cells cease division is unclear, as studies report mitotic arrest as early as cell cycle 15 (~8.5 hpf) for some notochordal cells (Kimmel et al., 1994), or widespread inhibition of mitosis in notochord by 28 hpf (Mendieta-Serrano et al., 2013).

By end of epiboly (yolk plug closure [YPC], 9 hpf), GM130 antibody-labeled GC had collected into fewer large puncta in the axial mesoderm, while in the nascent neuroectoderm, it remained more dispersed (Fig. 1G,H,J,K). By early segmentation stages (3–6 somites, 11–12 hpf), Golgi structures in axial and paraxial mesoderm cells had consolidated into one or a few compact patches (Fig. 1L,N–P,Q,T–U). Until the 5–6 somite stage, Golgi puncta in the neural ectoderm/plate remain in multiple fragments (Fig. 1B,H,M vs. R), when larger patches were observed in ventral neural plate cells.

In a parallel approach to visualize the GC, we injected synthetic RNA encoding GM130-tdTomato protein (Durdu et al., 2014) into single-celled zygotes and used confocal microscopy to observe live or fixed embryos. These experiments revealed a similar pattern of the GC dispersed in multiple fragments at earlier developmental stages in both ectoderm and mesoderm (early to mid-gastrulation, 6.5–8 hpf, Fig. 2A–D and data not shown). GM130

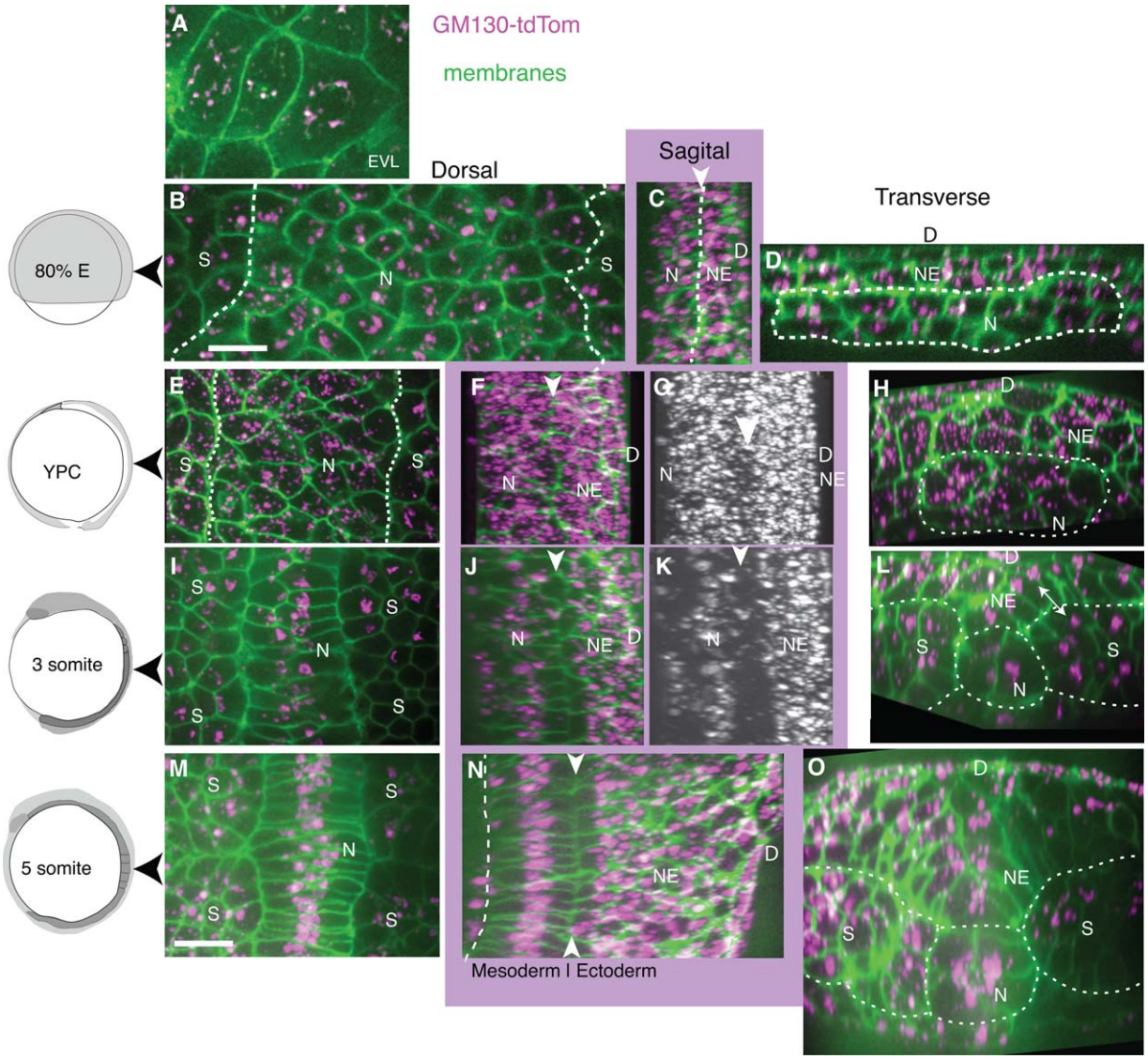

Fig. 2. Dynamic intracellular organization and position of the Golgi Complex revealed by GM130-TdTomato fusion protein during zebrafish gastrulation. Left column: Embryo age. **A–D**: Mid-gastrulation embryo (80% epiboly, 8.3 hpf). All images show Z-projection of GC shown on cell membrane from one plane, except as noted. A: EVL, z-projected 2 slices. B: Notochord and presomitic mesoderm, line at notochord/presomitic mesoderm boundary. C: Sagittal view of notochord and neuroectoderm with arrowhead and line between. D: Transverse view of notochord and neuroectoderm, line surrounding notochord. **E–H**: Late-gastrulation embryo (YPC, 9.5 hpf). E: Notochord and presomitic mesoderm, line at notochord/presomitic mesoderm boundary. F,G: Sagittal views. F: White arrowhead at notochord/neuroectoderm boundary. G: Z-projected GC, arrowhead indicates forming gap between notochord and neural plate. H: Transverse view, with line around notochord. **I–L**: 3 somite stage embryo, (11 hpf). I: Notochord and somites J,K: Sagittal views, white arrowhead at notochord/neuroectoderm boundary. L: Transverse view, line marks somites, notochord, and double arrowhead notes position of the GC in neural plate and somite cells. **M–O**: 5 somite stage embryo (11.7 hpf). M: Notochord and somites. N: Sagittal view, line marks ventral notochord and white arrowheads dorsal notochord. O: Transverse view, line marks boundaries of notochord, somites, and neural plate. N, notochord; NE, neuroectoderm or neural plate; S, somites; D, dorsal. Scale bars = 20 μm.

fluorescent protein labeling also corroborated the observation of gradual accumulation of the GC into larger complexes at later developmental stages. We observed fewer but larger Golgi patches in cells of the nascent notochord and somites (Fig. 2 E–O, YPC, 3 and 5 somite stages). However, there were also some differences between labeling with the fluorescent fusion protein and the antibody. Fluorescent GM130-tdTomato protein, while generating a brighter signal, displayed a more punctate pattern at YPC (9 hpf) relative to the endogenous antibody-labeled protein (compare Fig. 2E with Fig. 1G), particularly when the RNA dose was increased. Even when higher RNA doses were used, condensation and polarization of the GC were still observed (see Figure 5 A,B). Both methods may have limitations: An antibody may weakly label endogenous proteins or their phosphorylation and splice isoforms, thus not reveal all GC structures. Conversely, fusion protein expression is vulnerable to overexpression artifacts, like spottiness or labeling of incorrect subcellular compartments. Importantly, we observed that GM130 fusion protein signal was confined to the same intracellular regions as the antibody labeling.

Together these observations indicate that the GC is fragmented in mesenchymal mesoderm and ectoderm cells of mid-gastrulae with exception of forming Golgi ribbons in epithelial EVL cells. The GC consolidates into one major structure in notochordal cells at early segmentation stages.

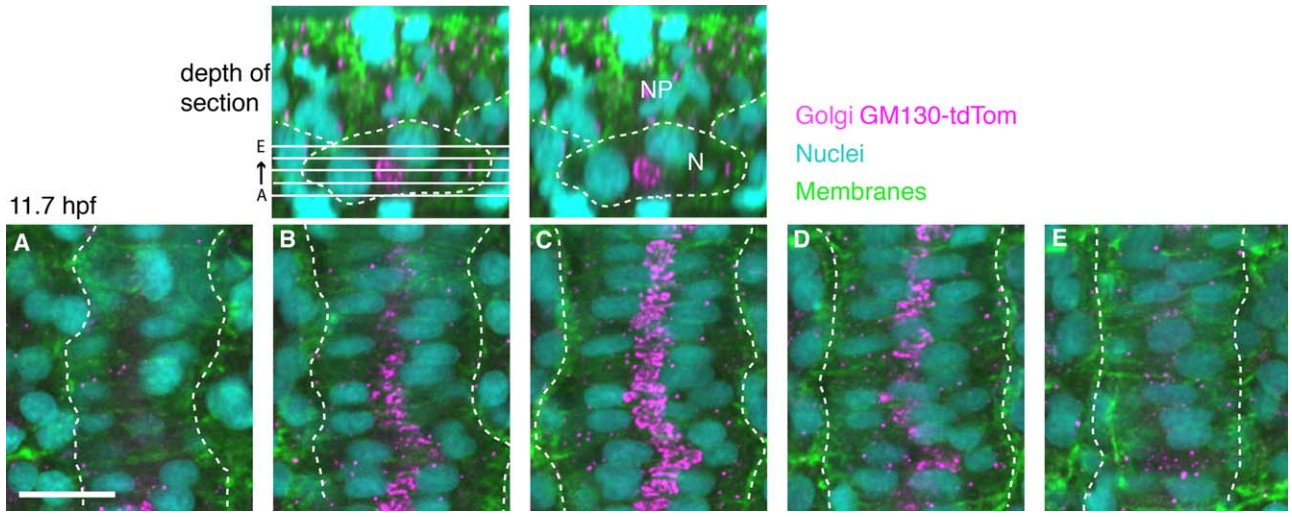

Fig. 3. The GC position relative to the nucleus in notochord cells. Top: Transverse views of dorsal side of 5 somite stage wild-type with notochord and somites outlined. Left: Location of sections. Right: Notochord (N), neural plate (NP). **A–E**: Confocal optical slices spaced 2.5 μm apart. GC (antibody to GM130, magenta), nuclei (DAPI, cyan), and cell membranes (green). Dotted white line highlights lateral edges of the notochord. Scale bar = 20 μm.

The Intracellular Position of Golgi Complex Becomes Polarized by Early Segmentation

By early segmentation stages (3–6 somites, 11–12 hpf), some tissues exhibited clear asymmetry of the GC intracellular location. GM130 antibody-labeled Golgi patches were positioned in notochord cells away from the boundary between notochord and adaxial mesoderm (Fig. 1L,N–P, Q,T,U and 2I–O). Likewise, in somite cells located at somitic furrows, the Golgi structures were found at the side opposite the furrow (Fig. 1L,Q, and 2I,L,M,O). The extent of the GC polarization in notochord cells was made more apparent when nuclei were labeled with DAPI in addition to GM130 antibody staining in 5 somite stage embryos (Fig. 3). We observed condensed Golgi patches in the center of the notochord, associated with the medial face of each cell nucleus, without apparent anterior-posterior bias (Fig. 3). Similar to the antibody labeling, GM130-tdTomato protein-labeled structures were positioned away from the notochord/somite boundary in notochord and adaxial mesoderm cells when viewed from dorsal (Fig. 2I,M). The extent of the GC intracellular polarization correlated with the extent of convergence of the notochord tissue (Fig. 4); that is, the notochords that converged to fewest cells in width also had cells exhibiting the most polarized GC. In addition, at 3 and 5 somite stages, the Golgi puncta localized away from the neuroectoderm-mesoderm boundary as seen in transverse and paraxial views of notochord and neuroectoderm (Fig. 2J–L,N,O).

To learn about the dynamic behavior of the GC during gastrulation, we acquired time-lapse movies of embryos in which GC and cell membranes were fluorescently labeled with GM130-tdTomato and GFP-CAAX respectively. To observe fast motions, we collected images at intervals of several seconds for a period of 10 minutes. Collecting such time-lapse movies at early gastrulation stages (6.5–8 hpf), we found that the Golgi fragments were mobile within mesodermal and ectodermal cells and did not fuse within a 10-minute observation period (data not shown). To observe long-term reorganization of the GC in cells, we collected images at intervals of minutes from late gastrulation (Fig. 5A,B, left) through early segmentation (Fig. 5A,B, right). These analyses revealed that Golgi puncta in the notochord cells gradually consolidated, over three hours, as was observed with antibody labeling of fixed embryos. Further, Golgi structures in the notochord and somites gradually moved away from the notochord/somite boundary (Fig. 5A,B). Taken together, these observations indicate that gastrula cells progress from a state characterized by a dispersed and unpolarized GC organization to one in which a more condensed Golgi ribbon, in nascent dorsal structures, is predictably located with respect to tissue boundaries.

Golgi Complex Puncta Contain Both Cis- and Trans-Golgi Proteins

To understand the nature of these dispersed Golgi puncta in gastrulating cells, we first considered if the dispersed nature of the Golgi structures could be explained by mitotic fragmentation. During mitosis the GC undergoes a stepwise disassembly to yield, first, laterally unlinked ministacks composed of cis- to trans-stacked cisternae, then unstacked cisternae, and finally simple vesicles (Colanzi and Sutterlin, 2013). We asked if the Golgi puncta we observed contained only proteins typical of one Golgi compartment (cis- vs. trans-Golgi cisternae) or contained both. In the former case, this would indicate single-type cisternae. If cis and trans markers co-localize, this would suggest these puncta are ministacks. As stacks are too small to easily distinguish with light microscopy (Flottmann et al., 2013), the formal possibility exists that co-localized markers indicate individual cisternae with mixed character. We think it more likely that the structures labeled with both cis and trans markers represent ministacks. To test the composition of puncta, we injected into single-celled zygotes a combination of synthetic RNAs encoding GM130-tdTomato (cis-Golgi resident protein) and GalT-GFP (galactose-1-phosphate uridylyltransferase, trans-Golgi resident protein) (Nilsson et al., 1993) and obtained confocal z-stacks and time-lapse movies between early gastrulation and 15 somite stage. Our initial time-lapse analyses revealed that Golgi puncta were mobile in the cells. Therefore, both fluorescent channels were collected before changing depth in the sample, to minimize potential artifactual displacement resulting from continuous movement of Golgi puncta. We found cis- and trans-Golgi markers nearly always co-localized in cells from

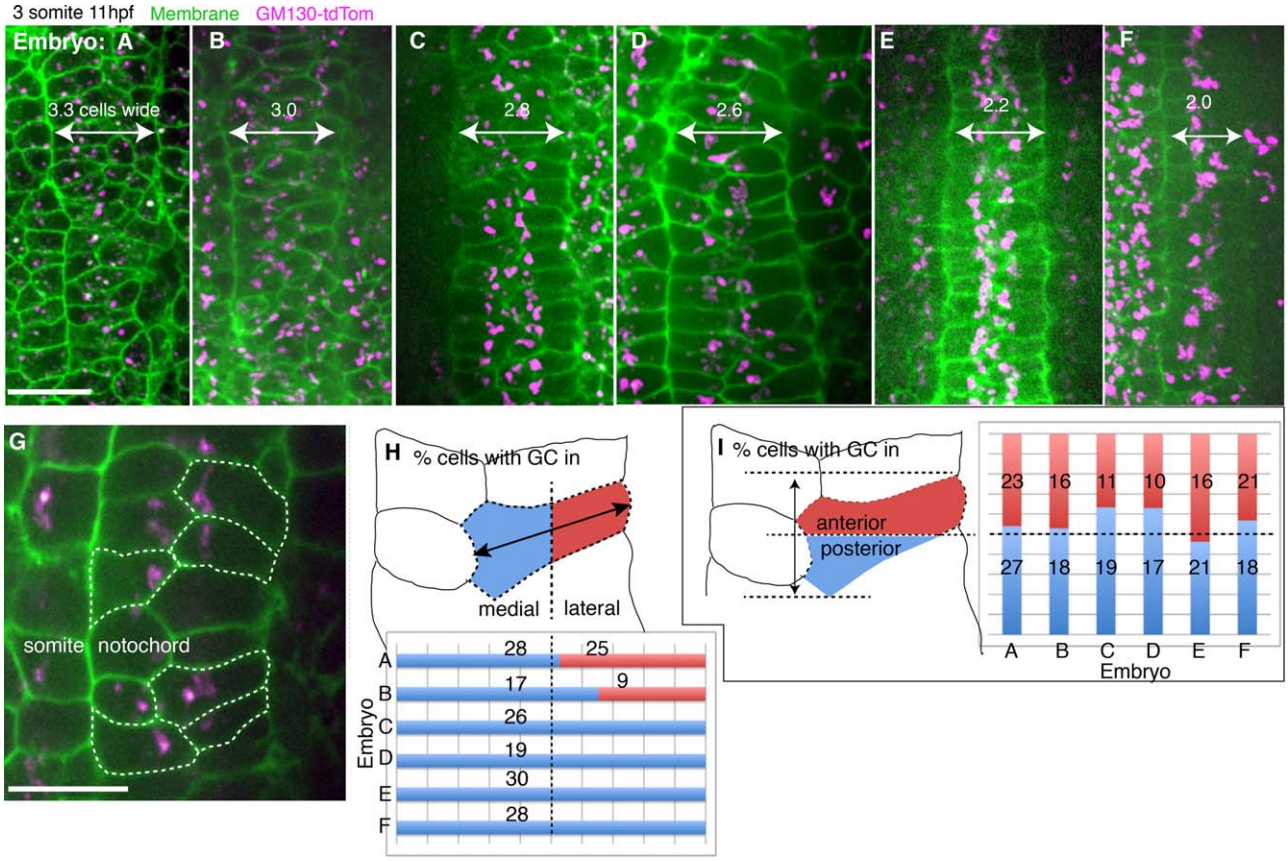

Fig. 4. Polarized intracellular location of the GC in 3 somite stage wild-type embryos. **A–F**: Images of GM130-TdTomato/membraneGFP expressing embryos, average width in cell number noted. G: Example of somite and notochord cells. H, top: Method for scoring presence of Golgi in medial and/or lateral region of cell. H, bottom: Percentage of cells with the GC in medial (blue) or lateral (red) region of notochord cell. Line is at 50% of cells. Numbers on bars indicate n = cells. I, left: Method for scoring presence of Golgi in anterior (red) and/or posterior (blue) half of cell. I, right: Percentage of cells with the GC in anterior and/or posterior region of notochord cell. Line is at 50% of cells. Numbers on bars indicate n = cells. Scale bar = 20 μm.

blastula through segmentation stages (98% at cleavage stages, 3–4 hpf, n = 4 embryos, 209 spots; 97.8% at 6.3 hpf, n = 2 embryos, 91 spots; 96.9% at 8.3 hpf, n = 5 embryos, 228 spots; 95.4% at 11 hpf, n = 2 embryos, 153 spots, Fig. 5C,D,F). We predicted that if cis- and trans-Golgi cisternae were co-localized, their movements should be concordant. Accordingly, in movies acquired at blastula and mid-gastrula stages (4–8 hpf, n = 2 embryos), we found that movements of the two Golgi compartment markers mimicked each other as could be seen in kymography (Fig. 5F). These results indicated the Golgi protein labeled puncta we observed represented stacked Golgi cisternae (ministacks) rather than unstacked cisternae or vesicles.

A Subset of Golgi Ministacks Associate With Centrosomes in Gastrulae Cells

In most dividing cells at the end of mitosis, dispersed Golgi vesicles track along MTs toward the centrosome and reassemble there into a Golgi ribbon (Thyberg and Moskalewski, 1999). We next addressed if any of the Golgi puncta in zebrafish gastrulae were associated with the centrosome, which would suggest Golgi vesicles bind to the centrosome and may move along the MT cytoskeleton. To address this, we injected one-cell stage embryos with synthetic RNAs encoding GM130-tdTomato, as well as a centrosome marker, GFP-Xcentrin (Piel et al., 2000; Sepich et al., 2011). We used Nomarski microscopy to distinguish individual cells, and confocal microscopy to observe fluorescently labeled centrosomes and Golgi structures in embryos from early gastrulation through early segmentation stages (6.3–11 hpf, Fig. 5E). We found that in most or all cells, one or two of the many GM130-labeled puncta overlapped or were adjacent to the GFP-Xcentrin-labeled centrosome (55.8% at early gastrulation, 7 hpf, n = 7 embryos, 238 cells; 79.9% at end of gastrulation, 9.5 hpf, n = 6 embryos, 200 cells; and 100% at early segmentation stages, 11 hpf and later, n = 5 embryos, 364 cells).

Taking these results together, we conclude that in cells of early zebrafish embryos, the cis-Golgi marker (GM130-tdTomato) co-localizes and co-migrates with a trans-Golgi marker (GalT-GFP), indicating that fluorescent puncta are Golgi ministacks. Additionally, one of the many Golgi puncta frequently co-localizes with the centrosome, suggesting association of the GC to centrosomes still occurs in cells with dispersed GC.

What Directs the Intracellular Positioning of the Golgi Complex?

To understand the cues guiding the observed polarization of Golgi structures in the notochord cells, we tested signals that might polarize the intracellular organelles within embryonic

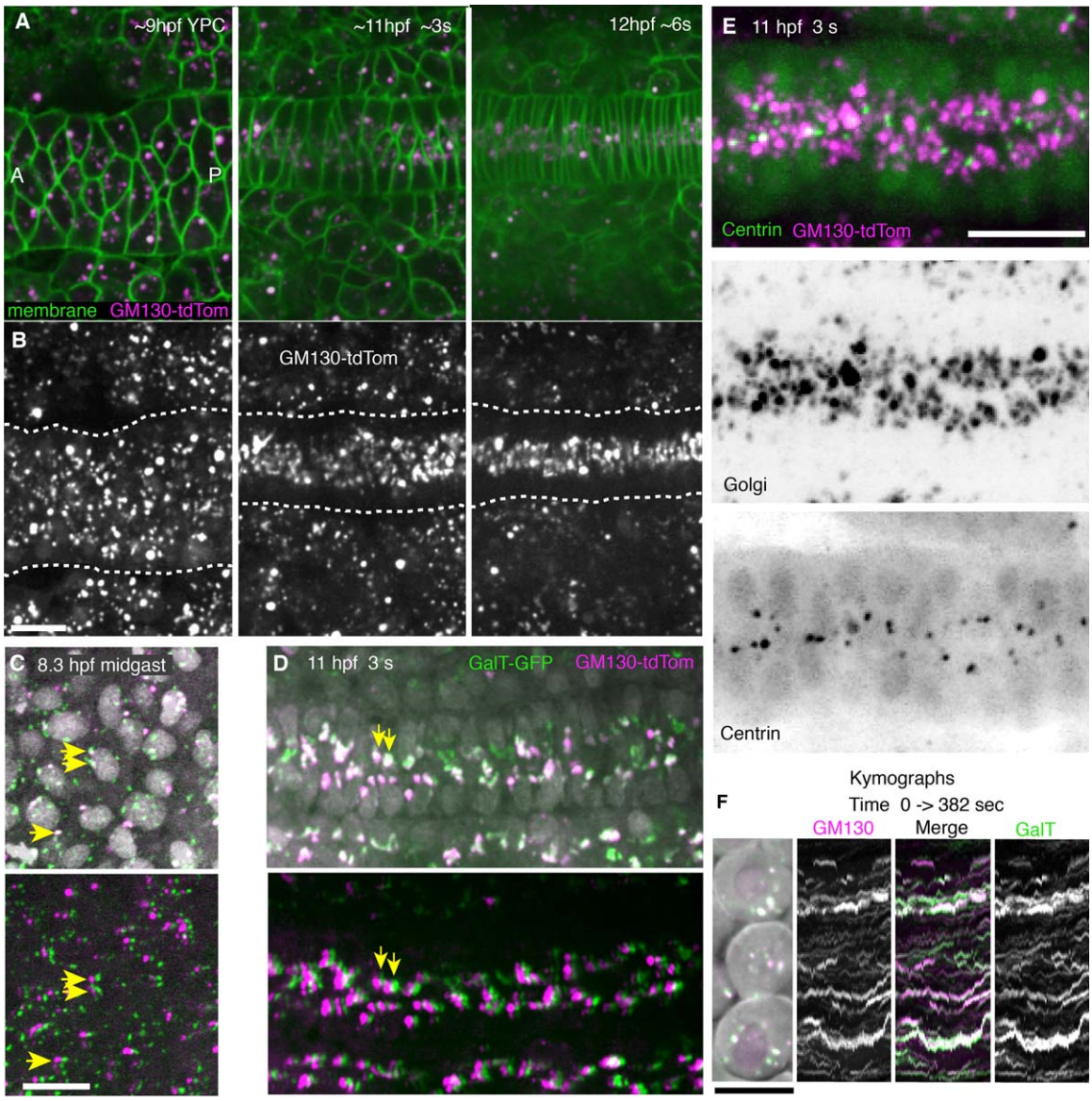

Fig. 5. Dynamic behavior of GC and co-localization of GM130 with GalT or centrosomes. **A,B**: Images from a time-lapse movie showing dynamic changes in GM130 distribution when the notochord converges and notochord cells become polarized. A: GM130 (cis-Golgi marker, magenta) and membrane-GFP (green). B: GM130 label alone. **C,D**: GM130 (cis-Golgi marker, magenta) and GalT (trans-Golgi marker, green) co-localize within the same Golgi bodies. Nuclei (gray). Yellow arrows indicate co-localized cis- and trans-Golgi puncta in top panel and same puncta shifted by ~2 μm in bottom panel to reveal co-localization of dim puncta. C: Mid-gastrulation, (80% epiboly, 8 hpf). C, top: GM130 and GalT with nuclei. C, bottom: GalT image shifted by ~2 μm. **D**: Early somitogenesis stage (3 somite, 11 hpf) showing notochord. D, top: GM130 and GalT with nuclei. D, bottom: GalT image shifted by ~2 μm. **E**: GC and centrosomes in notochord at 11 hpf (3 somite). E, top: Merged GFP-Xcentrin (green) and GM130tdTomato images (magenta). E, middle: Golgi (GM130). E, bottom: GFP-Xcentrin. **F**: Cells at 7 hpf (60% epiboly) expressing GM130 (magenta) and GalT (green). Kymographs from time-lapse movies of these cells show GC puncta from 0 to 382 seconds in movie. Ant, anterior; P, posterior. Scale bars = 20 μm.

tissues: Wnt/PCP, signals arising from the paraxial mesoderm and apical/basal polarity.

Wnt/PCP signaling is one of the key regulators of cellular polarity and coordination of polarity between cells within the plane of a tissue during gastrulation (Gray et al., 2011; Tada and Kai, 2012; Wallingford, 2012; Devenport, 2014). We previously reported that Wnt/PCP biases the centrosome to the posterior cell region during late-gastrulation C&E movements (Sepich et al., 2011). Due to the close association between some Golgi cisternae and the centrosome (Fig. 5E), we asked if Wnt/PCP signaling is required for the polarized position of the GC away from the notochord/somite boundary. To this end, we tested if two components of the Wnt/PCP signaling pathway were involved. The genes *frizzled7a* and *7b* (*fzd7a, fzd7b*) are zebrafish orthologs of the *Drosophila* core PCP gene *frizzled*, encoding seven-pass transmembrane receptors, inactivation of which produces a transient but striking C&E defect in zebrafish (Busch-Nentwich, 2010; Quesada-Hernandez et al., 2010). The gene *glypican4/knypek* (*gpc4/kny*) encodes a vertebrate-specific membrane-bound heparan sulfate proteoglycan, which promotes Wnt11/PCP signaling (Topczewski et al., 2001), antagonizes the Wnt inhibitor Dkk1 (Caneparo et al., 2007), and is essential for normal C&E

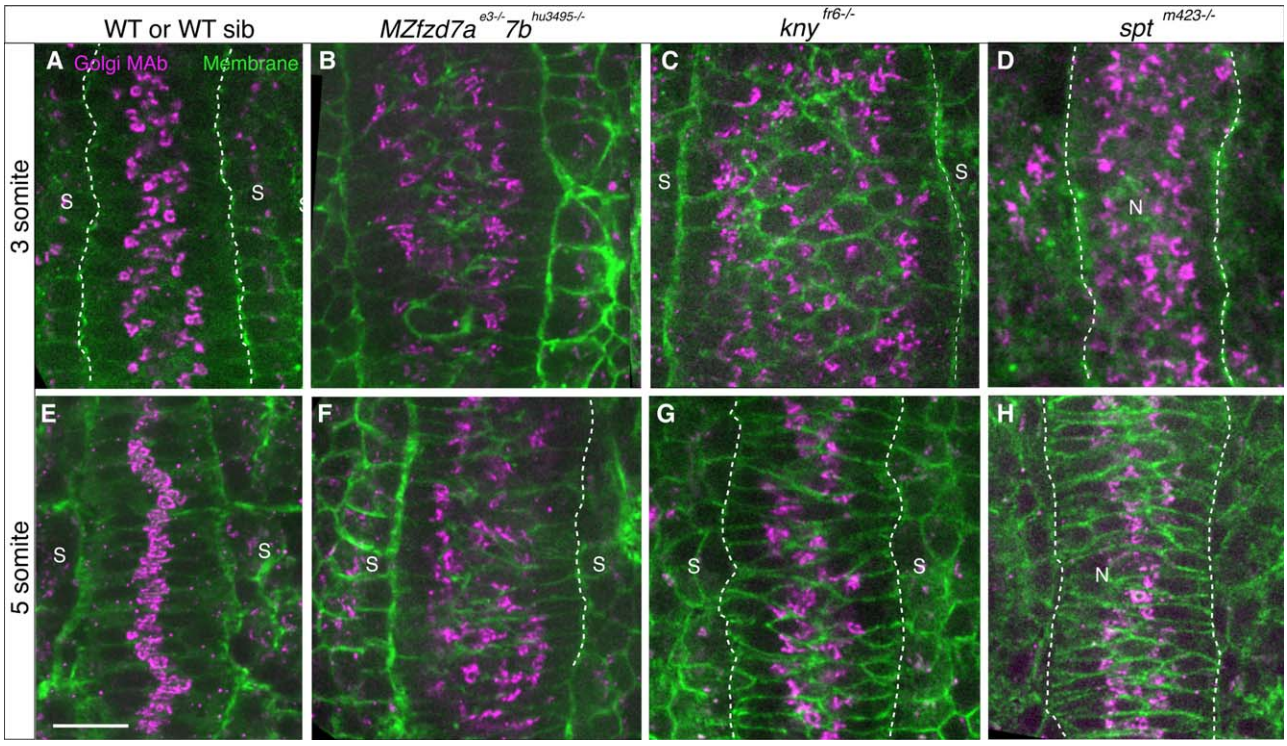

Fig. 6. Golgi Complex condensation and intracellular polarity in embryos deficient in Wnt/PCP signaling and somitic mesoderm. 3 somite (11 hpf) (**A–D**) and 5 somite stage (11.7 hpf) (**E–H**) embryos labeled with GM130 antibody (magenta) and cell membranes (green) A,E: WT (*spt* sibling). B,F: *fzd7a*$^{e3/e3}$;*fzd7b* $^{hu3495/}$. C,G: *kny*$^{fr6/fr6}$ D,H: *spt*$^{m423/m423.}$ Scale bars = 20 μm.

movements (Marlow et al., 1998). Embryos homozygous for nonsense mutations in *gpc4*/*kny* or *fzd7a*;*fzd7b* were examined at early somitogenesis stages for GC compaction and intracellular position in cells at the notochord/somite boundary. As expected, these mutant embryos displayed deficient C&E movements, resulting in a notochord that was mediolaterally wider in cell number than its wild-type (WT) counterpart (Fig. 6A,E vs. 6B,C,F,G), consistent with previous studies (Topczewski et al., 2001; Sumanas et al., 2002; Quesada-Hernandez et al., 2010). Despite this pronounced C&E defect, the GC formed compact patches in the notochord cells adjacent to the somites at early segmentation (Fig. 6B,C,F,G). Similar to our observations in WT embryos, the Golgi puncta in cells at the notochord/somite boundary were clearly positioned away from the boundary, whereas in internal cells, they showed no particular orientation (Fig. 6). These data indicate that, although Wnt/PCP signaling is required at this time and region for the cell polarity underlying normal C&E movements, normal Wnt/PCP signaling is not required for intracellular polarity of the GC in notochord and adaxial mesoderm cells.

What other cues might orient intracellular organelles during gastrulation? Several morphologic features of the notochord suggest it may be organized with an apical-basal epithelial polarity (Rodriguez-Boulan and Macara, 2014). Extracellular matrix is deposited on the outside of the notochord and remodeled during gastrulation movements in vertebrates (Yin and Solnica-Krezel, 2007; Davidson et al., 2008; Latimer and Jessen, 2010; Jessen, 2015). At early segmentation stages, notochord cells are shaped as flattened wedges partly spanning or disks fully spanning the notochord (Fig. 2I–O) with centrosomes located near the notochord center (Barrios et al., 2003). We reasoned that apical-basal polarity could provide such orientation cues for intracellular structures. To test if notochord cells are organized with an apical/basal polarity, we used an antibody against ZO1, a protein found apically in tight junctions (Stevenson et al., 1986). We found that at the 5 somite stage, ZO1 was expressed between cells of the EVL (Fig. 7A,C), an early-forming epithelial sheet, and in the ventral neural plate (Fig. 7A,B,D), but little or none was detected in the notochord (Fig. 7A,B,E). We interpret these observations to mean that the intracellular polarization of the Golgi structures in the notochord and adaxial cells does not depend on a fully formed epithelial organization with well developed tight junctions.

Signaling between precursors of the somites and notochord may provide orientation cues for the GC localization. The separation of the notochord from paraxial mesoderm is mediated in part by Eph/ephrin signaling, which stimulates local actinomyosin contractility to reduce cadherin intercellular adhesion. Local breakdown of adhesion drives separation between tissues bearing dissimilar sets of Eph/ephrin molecules (Fagotto et al., 2013). Eph/ephrin genes are expressed in similar patterns in zebrafish, suggesting Eph/ephrin signaling between paraxial mesoderm and notochord could guide boundary formation (Thisse, 2005). We asked if paraxial mesoderm and/or nascent somites provided a molecular or mechanical signal to the notochord that could account for the striking polarization of the Golgi structures away from the boundary in the notochord cells. To this end, we analyzed *spadetail* (*spt*/*tbx16*$^{m423/m423}$) mutant embryos lacking the T-box transcription factor Tbx16. In these mutants, lateral and ventral mesoderm migrate abnormally during gastrulation and subsequently fail to form somites flanking the notochord (Ho and Kane, 1990; Row et al., 2011). In *spt*/*tbx16*$^{m423/m423}$ mutant

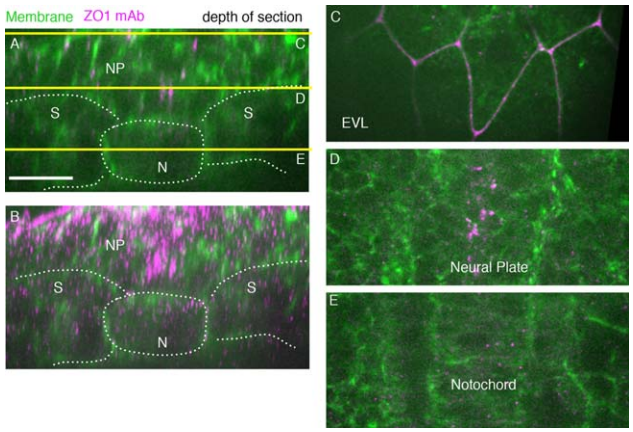

Fig. 7. ZO1 antibody-labeled tight junctions in 5 somite stage wild-type embryo (11.7 hpf). A: A single-transverse-plane ZO1 antibody (magenta) cell membranes (green, Transgene [*actb::Myosinl12-GFP*]). Yellow lines show depth of sections in C,D,E. Dorsal is to the top. Lines mark tissue boundaries. **B**: Transverse z-projected section of wild-type embryo (*spt* sibling). **C**: EVL cells. **D**: Ventral neural plate. **E**: Notochord. N, notochord; NP, neural plate; S, somites. Scale bars = 20 μm.

embryos (Solnica-Krezel et al., 1996), Golgi puncta condensed in notochord cells into compact patches, which were positioned away from the notochord/somite boundary at the 3 and 5 somite stages (Fig. 6D,H). These results indicate that the mechanisms that condense and polarize the Golgi structures in notochord cells do not depend on Wnt/PCP signaling, signals from the forming somites, or mature epithelial organization.

Discussion

Golgi Complex is Dispersed in Cells at Early Developmental Stages; Later Condenses and Becomes Intracellularly Polarized

A condensed and polarized Golgi Complex is necessary for directed migration in cultured cells (Drabek et al., 2006; Yadav et al., 2009; Sanders and Kaverina, 2015). It is not clear whether polarized and condensed GC is required during gastrulation cell movements. We report that the architecture of the GC changes from dispersed bodies at early gastrulation to a condensed form in select cell types at mid-gastrulation and early somitogenesis. When cells function as cohorts or tissues, they coordinate their behaviors and structures through shared polarity, notably mediated by apical-basal and planar cell polarity. Intracellular polarization of GC has been reported for cells in mature epithelial organs (Kreft et al., 2010; Gunn et al., 2011). Whether similar GC polarity emerges during embryogenesis is not known. Here, we describe intracellular and intercellular polarity that arise in the vertebrate embryo as germ layers organize into tissues and organs during embryogenesis. With the exception of the superficial epithelial EVL, the GC remained dispersed until segmentation stages, when GC condensed around the centrosome, and showed clear polarization in cells located at notochord and somite tissue boundaries. This polarization was independent of Wnt/PCP signaling, cues provided by somites, and mature apical/basal polarity.

Functions of Dispersed GC and Factors Triggering Condensation

Is a condensed Golgi ribbon required for directed cell migration in zebrafish gastrulae? In light of the requirement in migrating cultured cells for condensed, polarized GC (Drabek et al., 2006; Yadav et al., 2009; Hurtado et al., 2011), we were surprised to find that the GC was dispersed into several bodies in cells of young zebrafish gastrulae in which massive cell movements and rearrangements take place. We followed the transition from dispersed to compact GC architecture and polarization relative to tissue boundaries by labeling with an antibody to GM130, a cis-Golgi resident protein, and labeling by injection of synthetic RNAs encoding fluorescently tagged GM130 and GalT proteins. We found GC in dispersed bodies at early gastrulation and in a condensed form in select cell types at mid-gastrulation and early somitogenesis, and most or all cells by 24 hpf (data not shown).

While the textbook representation of the cell includes a juxtanuclear compact Golgi ribbon, this architecture is far from universal. A dispersed GC arrangement, as we report here for zebrafish gastrulae, has been observed in wide varieties of organisms, including insects, plants, and budding yeast (Thyberg and Moskalewski, 1999). Some organisms transition from dispersed to compact GC forms (Yano et al., 2005; Kondylis and Rabouille, 2009). A similar GC condensation was reported for the sea urchin embryo (*L. variegatus*), with the transition at the ninth cell cleavage (Terasaki, 2000). In younger *Drosophila* tissues (from syncytial embryos to larval imaginal discs), the GC is distributed in vesicles (Ripoche et al., 1994; Kondylis et al., 2001). By pupal stages, the GC condenses into a pair of stacks in each cell. Interestingly, in *Drosophila* this remodeling is dependent on exposure to an external signal, ecdysone, the hormone essential for larval to pupal transition (Kondylis et al., 2001). In contrast, other organisms exhibit condensed GC at early developmental stages, e.g., mouse embryos by the 32-cell blastocyst stage (E3.5) (Kim et al., 2012) and dispersed GC forms later in specific cell types. Mouse gastric parietal cells, responsible for production of stomach acid, have GC with a dispersed organization, whereas neighboring non-parietal cells display Golgi ribbons (Gunn et al., 2011). Similarly, when porcine uroepithelial cells differentiate, their GC remodels from a juxtanuclear ribbon to dispersed fragments near the apical surface (Kreft et al., 2010). GC architecture is dynamic and is regulated in a stage and cell type–specific manner.

Does Golgi architecture affect its function? In the gastric and uroepithelial secretory cells described above, the authors favor the idea that the dispersed GC provides superior secretory function (Kreft et al., 2010; Gunn et al., 2011). However, work from several labs argues that a condensed and polarized Golgi ribbon is essential for directed secretion and directed motility in primary fibroblasts and immortalized epithelial cells (Schmoranzer et al., 2003; Miller et al., 2009; Yadav et al., 2009; Hurtado et al., 2011). When ribbon assembly was blocked, these cells had normal global secretion but impaired directed protein trafficking to the leading edge and directed migration (Schmoranzer et al., 2003; Yadav et al., 2009; Hurtado et al., 2011). Finally, the hypothesis has been advanced that a juxtanuclear compact GC is important for the polarized cell state (Yadav and Linstedt, 2011).

In our studies, we observed dispersed GC by antibody labeling during blastula and gastrulation stages. The first tissue in which we observed compact GC was the EVL at mid-to-late gastrulation

(8.3–9 hpf) (Slanchev et al., 2009 and Fig. 1C). Before GC accumulates around the nucleus, the EVL is capable of critical functions, including forming a flattened epithelial sheet covering the embryo (2.7 hpf, 512 cell stage) (Kimmel et al., 1990; Zhang et al., 2011), serving as an osmotic barrier (4.7 hpf, 30% epiboly) (Kiener et al., 2008; Fukazawa et al., 2010), and participating in the gastrulation movement of epiboly (4.3 hpf) (Kimmel et al., 1995). At the time these processes occur, EVL cells have a dispersed GC, suggesting that a compact architecture is not required. The formation of a perinuclear condensed GC probably does not correspond to final differentiation, as the EVL subsequently contributes to the outer layer of the skin (14 hpf) (Slanchev et al., 2009). We also observed dispersed GC in the notochord and the adjacent adaxial mesoderm during gastrulation when these tissues function in body elongation (Solnica-Krezel, 2005), as well as secretion of Nodal and Hedgehog signals (Krauss et al., 1993; Tian et al., 2003). The GC became compact before notochord cells vacuolated, driving further extension of the body axis (17–20 hpf) (Dale and Topczewski, 2011; Ellis et al., 2013). As gastrulation entails extensive and varied cell movements and rearrangements and cell fate specifications (Solnica-Krezel, 2005), these observations argue that in zebrafish embryonic cells, a dispersed GC organization is compatible with directed cell motility and fate acquisition.

In our studies, the architecture of the GC changed at distinct developmental stages and in a cell type–specific manner. One could imagine that a short cell cycle might preclude reassembly of a condensed GC ribbon. While cell division often regulates the architecture of the GC (Yadav and Linstedt, 2011), we think it is unlikely that mitosis itself accounts for the dispersed nature of the GC during gastrulation. In embryonic zebrafish, cells cleave rapidly (~20 minutes) and synchronously until about 3 hpf, when the cell cycle begins to lengthen. However, the onset of condensed and polarized GC organization, in EVL at 8 hpf, only roughly correlates with lengthening of the cell cycle by early gastrulation (5 hpf, about cell cycle 13, 54 minutes) (Kane and Kimmel, 1993). Further, during mitotic fragmentation in cultured cells, Golgi cisternae unstack and separate into vesicles, and protein transport is arrested (Colanzi and Sutterlin, 2013). We observed GC puncta appear to cluster around daughter centrosomes when cells divided, but we did not observe GC becoming more condensed at any particular time within one cell cycle. If GC in embryonic zebrafish cells was dispersed by mitosis, then markers of cis- and trans-Golgi compartments should be found either in separate puncta or spread as a haze over the cell. Instead, we found co-localization of markers of the cis- and trans-Golgi compartments, GM130 and GalT, respectively, strongly suggesting that dispersed Golgi puncta are miniature stacks of cisternae. The presence of Golgi ministacks and timing of increase in the cell cycle argue that a dispersed Golgi Complex is not the result of incomplete resolution of normal mitotic GC dispersal.

Related to cell cycle lengthening is the idea of fate acquisition following cessation of cell division. According to this model, EVL and notochord acquire condensed Golgi as an aspect of partial or complete differentiation. Supporting this are reports that both cell types slow or stop dividing before GC condensation (EVL at about 5–6 hpf; some notochord cells as early as mid-gastrulation [8.5 hpf]; others as late as 28 hpf) (Kane, 1999; Jiang and Smith, 2007; Mendieta-Serrano et al., 2013). As noted above, the EVL is the first tissue to form an epithelial sheet at 2.7 hpf, with barrier function by 4.7 hpf.

An experimental perturbation reported to disperse the GC suggests a potential mechanism for maintaining a dispersed GC. Reassembly of the Golgi ribbon at the end of mitosis requires movement of Golgi vesicles on MT toward the centrosome, and inhibition of this movement scatters the GC. Transport of Golgi vesicles depends on dynein/dynactin motor complex, intact MTs, and cargo adaptors on Golgi vesicles (Schmoranzer et al., 2003; Hurtado et al., 2011; Yadav and Linstedt, 2011; Yadav et al., 2012). The dispersed GC state in zebrafish embryonic cells might be explained if Golgi fragments were unable to track along MTs toward the centrosome. Consistent with this notion, we usually observed dispersed GC in the cytoplasm, while one Golgi body was found at the centrosome. Hence, at least some Golgi structures can interact with MTs and accumulate near centrosome, while others cannot. The GC might be held in a dispersed state in zebrafish embryos if they are unable to interact with MTs.

Our interpretation of these data is that a dispersed GC is a normal form for zebrafish embryos during cleavage and gastrula stages, and dispersion is compatible with cell migration and fate acquisition. The dispersed state is maintained, perhaps, by a mechanism as simple as inhibition of proteins involved in Golgi interaction with MT motors. The dispersed GC bodies condense at the centrosome likely in response to cell type–specific signals. These signals occur after cell cycle slows and may be the phenotype of these partly differentiated cells.

Intracellular Polarity of Compact Golgi Complex

We report intracellular and intercellular polarity that arises in the vertebrate embryo as germ layers organize into tissues and organs during embryogenesis. With the exception of the superficial epithelial EVL, the GC remained dispersed until segmentation stages, when GC condensed around the centrosome, and showed clear polarization in cells located at notochord and somite tissue boundaries. We observe that as GC condensed it became polarized within cells. This is most striking in the cells of the somites and at the boundary between somite and notochord (Fig. 1L–U, 2I–O). We tested several potential signaling systems as the trigger for Golgi polarization: Wnt/PCP signaling, cues provided by somites, and mature apical/basal polarity.

Wnt/PCP signaling is a critical regulator of planar cell polarity during C&E gastrulation movements in vertebrates (Gray et al., 2011) and influences cell movements and orientations in the axial and paraxial mesoderm during gastrulation. However, here we found that embryos lacking Wnt/PCP components Frizzled 7a and 7b or Glypican4 had oriented GC in cells on the notochord/somite boundary (Fig. 6A–C,E–G). These results show that Wnt/PCP signaling is not required for intracellular localization of the GC in notochord boundary cells.

Eph/ephrin signaling at least partly drives the separation of notochord and paraxial mesoderm in *Xenopus* (Park et al., 2011; Fagotto et al., 2013; Fagotto et al., 2014; Rohani et al., 2014). Such a boundary might provide a signal to polarize the GC in the notochord. We examined notochords in *tbx16/spt* mutants, which lack presomitic mesoderm and, thus, signals generated by paraxial mesoderm. However, we found that cells at the edge of the notochord exhibited polarized GC distribution in *tbx16/spt* mutant embryos (Fig. 6D–H). This result shows that GC positioning does not depend on signals derived from the paraxial

mesoderm. Further, this result suggests that polarity within the notochord depends on interactions between notochord cells themselves.

The polarized position of GC may be an aspect of growing epithelialization within the notochord and somites of segmentation-stage zebrafish embryos. A typical epithelial cell has cilium, centrosome, Golgi structures, and nucleus arranged from apical to basal, with tight junctions containing ZO1 found at the transition between apical and basolateral domains (Rodriguez-Boulan and Macara, 2014). Early segmentation–stage zebrafish notochord cells exhibited an intracellular arrangement that resembled that of an epithelial cell; centrosomes and GC were located centrally with nuclei located peripherally (Fig. (3 and 5)). However, our studies did not find mature apical/basal polarity in the notochord or adaxial mesoderm associated with polarized GC localization. Instead, we detected no notochord regions with ZO1-labeled tight junctions, contrasting strong ZO1 labeling seen between EVL cells and between cells of the ventral neural tube at early segmentation stages (Fig. 7). These results indicate that GC orientation does not follow the establishment of mature apical/basal polarity. However, we cannot exclude the possibility that nascent apical/basal polarity in the notochord cells underlies the observed GC positioning.

Two additional processes seem relevant as mechanisms to potentially polarize the GC. Once GC condenses at the centrosome, influences on the centrosome may determine their conjoined position (Yadav and Linstedt, 2011; Elric and Etienne-Manneville, 2014). Studies of migrating cultured cells propose that external cues locally activate a Cdc42/Par6/aPKC polarity complex to recruit and bind dynein/dynactin motors at the membrane. Motor activity then exerts pulling force on captured MTs, consequently moving the centrosome and attached GC. It is therefore intriguing that we observed polarization of the GC when it was condensed and when it was co-localized with the centrosome. Second, Cadherin adhesion between cells in vitro or in vivo may orient the centrosomes (Desai et al., 2009; Dupin et al., 2009; Revenu et al., 2014). In small colonies of cells grown on micropatterns, intracellular organelles orient relative to internal cell-cell contacts and non-adhesive free edges. Establishment and maintenance of this polarity is dependent on cadherin adhesion between cells. We hypothesize that mechanisms like these underlie the dynamic changes in the GC intracellular organization during zebrafish gastrulation.

Our interpretations of these data are that the intracellular position of the compact GC is a manifestation of the intracellular polarity and organization of the notochord and somites. This organization places centrosomes and GC in the center of the tissue with nuclei toward the organ surface. Both the GC compaction and positioning may be guided by cell type–specific signals during zebrafish gastrulation and early segmentation, and may depend on cell interactions within each tissue. These signals are independent of Wnt/PCP or signals arising from the paraxial mesoderm and do not require mature apical/basal polarity.

Experimental Procedures

Fish

Embryos were obtained from natural spawnings using the following lines: AB*, Tu x AB*, *Tg[actb::Myl12.1-EGFP]*^{e2212} (Ruprecht et al., 2015), *knypek*^{fr6} (Topczewski et al., 2001), *spadetail*^{m423} (Solnica-Krezel et al., 1996)), or *frizzled fzd7a*^{e3}*;fzd7b* ^{hu3495} (Busch-Nentwich, 2010; Quesada-Hernandez et al., 2010). Embryos were raised at 28°C or 32°C according to time considerations and staged according to morphology (Kimmel et al., 1995). All protocols were approved by and follow the guidelines of the Institutional Animal Care and Use Committee at Washington University School of Medicine.

Imaging, Antibodies, and Fluorescent Fusion Proteins

All images of live and fixed embryos were collected with a spinning disk confocal microscope (Quorum, Canada) using an inverted Olympus IX-81 microscope, a Hamamatsu EMCCD camera (C9100-13), and Metamorph acquisition software. Images of GM130 MAb labeling were collected using an Olympus 60x (N.A. 1.15) water immersion objective. Images of GM130-tdTomato were collected using an Olympus 40x (N.A. 0.75) air objective. Images were analyzed using Fiji/ImageJ (Schindelin et al., 2012). Virtual transverse and parasagittal sections were made as orthogonal reconstructions using the Image/Stacks/Reslice function in Fiji/ImageJ. If embryos were tilted in z-stacks, they were turned using Fiji/Stacks/Reslice and Fiji/Transform/Rotate.

Antibodies were used at the following dilutions: GM130 (BD Transduction Labs, #610822, 1:500), ZO1 (Zymed Laboratories Inc., cat.#33-9100,1:200), β-catenin (Santa Cruz Biotechnology Inc., #H102, 1:200). Life Technologies supplied Alexa488 goat anti-mouse (#A11029, 1:500), Alexa647 goat anti-mouse (#A21235, 1:500), Alexa568 goat anti-rabbit (#A11036, 1:500), Alexa568-phalloidin (#A12380, 1:500), or Alexa647-Phalloidin (#A22287, 1:500). Immunohistochemistry was performed according to Wu et al. (Wu et al., 2012) with modifications. Embryos were permeabilized in 0.5% Triton X-100 in Phosphate Buffered Saline (PBS) for 20 or 60 minutes (m, younger than 9 hpf vs. older). Washes used 0.1% Triton X-100 in PBS (PBSTr), and blocking and antibody incubation used AB solution (PBSTr, 1% DMSO, 2% BSA, 5% goat serum). GM130 antibody was incubated with embryos for 48 hr at 4°C.

For fusion proteins, embryos were injected at the 1 cell stage with synthetic RNA at the following doses: membrane localized GFP-CAAX (100–300 pg) and GM130-tdTomato (15–150 pg), or GalT-GFP (galactose-1-phosphate uridylyltransferase, 13–60 pg) and membraneRFP or membraneCherry (200 pg), GFP-*Xenopus* centrin or Cherry-*Xenopus* centrin 10 pg, or Histone2B-RFP (H2B) at 15 pg. H2B-TagBFP (Addgene) at 50 pg was toxic in our hands. Doses of GM130 above 250 pg caused a low rate of cyclopia (data not shown). Embryos were imaged live or fixed.

Acknowledgments

We thank Terin Budine, Gina Castelvecchi, Yinzi Liu, Margot Williams, and Isa Roszko for commenting on the manuscript. We thank C-P Heisenberg for GM130-tdTomato, Kristin Kwan for GFP-Xcentrin, and George Patterson for GalT-GFP. Authors have no financial conflicts of interest.

References

Barrios A, Poole RJ, Durbin L, Brennan C, Holder N, Wilson SW. 2003. Eph/Ephrin signaling regulates the mesenchymal-to-epithelial transition of the paraxial mesoderm during somite morphogenesis. Curr Biol 13:1571–1582.

Blankenship JT, Backovic ST, Sanny JS, Weitz O, Zallen JA. 2006. Multicellular rosette formation links planar cell polarity to tissue morphogenesis. Dev Cell 11:459–470.

Busch-Nentwich E, Kettleborough, R., Fenyes, F., Herd, C., Collins, J., Winkler, S., Brand, M., de Bruijn, E., van Eeden, F., Cuppen, E., and Stemple, D.L. 2010. Sanger Institute Zebrafish Mutation Resource targeted knock-out mutants phenotype and image data submission. In: ZFIN Direct Data Submission (http://zfin.org).

Caneparo L, Huang YL, Staudt N, Tada M, Ahrendt R, Kazanskaya O, Niehrs C, Houart C. 2007. Dickkopf-1 regulates gastrulation movements by coordinated modulation of Wnt/beta catenin and Wnt/PCP activities, through interaction with the Dally-like homolog Knypek. Genes Dev 21:465–480.

Colanzi A, Sutterlin C. 2013. Signaling at the Golgi during mitosis. Methods Cell Biol 118:383–400.

Dale RM, Topczewski J. 2011. Identification of an evolutionarily conserved regulatory element of the Zebrafish col2a1a gene. Dev Biol 357:518–531.

Davidson LA, Dzamba BD, Keller R, Desimone DW. 2008. Live imaging of cell protrusive activity, and extracellular matrix assembly and remodeling during morphogenesis in the frog, Xenopus laevis. Dev Dyn 237:2684–2692.

Desai RA, Gao L, Raghavan S, Liu WF, Chen CS. 2009. Cell polarity triggered by cell-cell adhesion via E-cadherin. J Cell Sci 122: 905–911.

Devenport D. 2014. The cell biology of planar cell polarity. J Cell Biol 207:171–179.

Drabek K, van Ham M, Stepanova T, Draegestein K, van Horssen R, Sayas CL, Akhmanova A, Ten Hagen T, Smits R, Fodde R, Grosveld F, Galjart N. 2006. Role of CLASP2 in microtubule stabilization and the regulation of persistent motility. Curr Biol 16: 2259–2264.

Dupin I, Camand E, Etienne-Manneville S. 2009. Classical cadherins control nucleus and centrosome position and cell polarity. J Cell Biol 185:779–786.

Durdu S, Iskar M, Revenu C, Schieber N, Kunze A, Bork P, Schwab Y, Gilmour D. 2014. Luminal signalling links cell communication to tissue architecture during organogenesis. Nature 515: 120–124.

Efimov A, Kharitonov A, Efimova N, Loncarek J, Miller PM, Andreyeva N, Gleeson P, Galjart N, Maia AR, McLeod IX, Yates JR, 3rd, Maiato H, Khodjakov A, Akhmanova A, Kaverina I. 2007. Asymmetric CLASP-dependent nucleation of noncentrosomal microtubules at the trans-Golgi network. Dev Cell 12:917–930.

Ellis K, Bagwell J, Bagnat M. 2013. Notochord vacuoles are lysosome-related organelles that function in axis and spine morphogenesis. J Cell Biol 200:667–679.

Elric J, Etienne-Manneville S. 2014. Centrosome positioning in polarized cells: common themes and variations. Exp Cell Res 328:240–248.

Etienne-Manneville S. 2013. Microtubules in cell migration. Annu Rev Cell Dev Biol 29:471–499.

Fagotto F, Rohani N, Touret AS, Li R. 2013. A molecular base for cell sorting at embryonic boundaries: contact inhibition of cadherin adhesion by ephrin/Eph-dependent contractility. Dev Cell 27:72–87.

Fagotto F, Winklbauer R, Rohani N. 2014. Ephrin-Eph signaling in embryonic tissue separation. Cell Adh Migr 8:308–326.

Fanto M, McNeill H. 2004. Planar polarity from flies to vertebrates. J Cell Sci 117:527–533.

Flottmann B, Gunkel M, Lisauskas T, Heilemann M, Starkuviene V, Reymann J, Erfle H. 2013. Correlative light microscopy for high-content screening. Biotechniques 55:243–252.

Fukazawa C, Santiago C, Park KM, Deery WJ, Gomez de la Torre Canny S, Holterhoff CK, Wagner DS. 2010. poky/chuk/ikk1 is required for differentiation of the Zebrafish embryonic epidermis. Dev Biol 346:272–283.

Godde NJ, Galea RC, Elsum IA, Humbert PO. 2010. Cell polarity in motion: redefining mammary tissue organization through EMT and cell polarity transitions. J Mammary Gland Biol Neoplasia 15:149–168.

Goodrich LV, Strutt D. 2011. Principles of planar polarity in animal development. Development 138:1877–1892.

Gray RS, Roszko I, Solnica-Krezel L. 2011. Planar cell polarity: coordinating morphogenetic cell behaviors with embryonic polarity. Dev Cell 21:120–133.

Gunn PA, Gliddon BL, Londrigan SL, Lew AM, van Driel IR, Gleeson PA. 2011. The Golgi apparatus in the endomembrane-rich gastric parietal cells exist as functional stable mini-stacks dispersed throughout the cytoplasm. Biol Cell 103:559–572.

Guo Y, Zanetti G, Schekman R. 2013. A novel GTP-binding protein-adaptor protein complex responsible for export of Vangl2 from the trans Golgi network. Elife 2:e00160.

Haigo SL, Hildebrand JD, Harland RM, Wallingford JB. 2003. Shroom induces apical constriction and is required for hingepoint formation during neural tube closure. Curr Biol 13:2125–2137.

Hale R, Strutt D. 2015. Conservation of Planar Polarity Pathway Function Across the Animal Kingdom. Annu Rev Genet 49:529–551.

Hay ED. 2005. The mesenchymal cell, its role in the embryo, and the remarkable signaling mechanisms that create it. Dev Dyn 233:706–720.

Ho RK, Kane DA. 1990. Cell-autonomous action of Zebrafish spt-1 mutation in specific mesodermal precursors. Nature 348:728–730.

Hurtado L, Caballero C, Gavilan MP, Cardenas J, Bornens M, Rios RM. 2011. Disconnecting the Golgi ribbon from the centrosome prevents directional cell migration and ciliogenesis. J Cell Biol 193:917–933.

Jessen JR. 2015. Recent advances in the study of Zebrafish extracellular matrix proteins. Dev Biol 401:110–121.

Jessen JR, Topczewski J, Bingham S, Sepich DS, Marlow F, Chandrasekhar A, Solnica-Krezel L. 2002. Zebrafish trilobite identifies new roles for Strabismus in gastrulation and neuronal movements. Nat Cell Biol 4:610–615.

Jiang D, Smith WC. 2007. Ascidian notochord morphogenesis. Dev Dyn 236:1748–1757.

Kane DA. 1999. Cell cycles and development in the embryonic Zebrafish. Methods Cell Biol 59:11–26.

Kane DA, Kimmel CB. 1993. The Zebrafish midblastula transition. Development 119:447–456.

Kiener TK, Selptsova-Friedrich I, Hunziker W. 2008. Tjp3/zo-3 is critical for epidermal barrier function in Zebrafish embryos. Dev Biol 316:36–49.

Kim S, Hill A, Warman ML, Smits P. 2012. Golgi disruption and early embryonic lethality in mice lacking USO1. PLoS One 7: e50530.

Kimmel CB, Ballard WW, Kimmel SR, Ullmann B, Schilling TF. 1995. Stages of embryonic development of the Zebrafish. Dev Dyn 203:253–310.

Kimmel CB, Warga RM, Kane DA. 1994. Cell cycles and clonal strings during formation of the Zebrafish central nervous system. Development 120:265–276.

Kimmel CB, Warga RM, Schilling TF. 1990. Origin and organization of the Zebrafish fate map. Development 108:581–594.

Kinoshita N, Sasai N, Misaki K, Yonemura S. 2008. Apical accumulation of Rho in the neural plate is important for neural plate cell shape change and neural tube formation. Mol Biol Cell 19:2289–2299.

Kondylis V, Goulding SE, Dunne JC, Rabouille C. 2001. Biogenesis of Golgi stacks in imaginal discs of Drosophila melanogaster. Mol Biol Cell 12:2308–2327.

Kondylis V, Rabouille C. 2009. The Golgi apparatus: lessons from Drosophila. FEBS Lett 583:3827–3838.

Krauss S, Concordet JP, Ingham PW. 1993. A functionally conserved homolog of the Drosophila segment polarity gene hh is expressed in tissues with polarizing activity in Zebrafish embryos. Cell 75:1431–1444.

Kreft ME, Di Giandomenico D, Beznoussenko GV, Resnik N, Mironov AA, Jezernik K. 2010. Golgi apparatus fragmentation as a mechanism responsible for uniform delivery of uroplakins to the apical plasma membrane of uroepithelial cells. Biol Cell 102: 593–607.

Latimer A, Jessen JR. 2010. Extracellular matrix assembly and organization during Zebrafish gastrulation. Matrix Biol 29:89–96.

Levayer R, Lecuit T. 2013. Oscillation and polarity of E-cadherin asymmetries control actomyosin flow patterns during morphogenesis. Dev Cell 26:162–175.

Lim J, Thiery JP. 2012. Epithelial-mesenchymal transitions: insights from development. Development 139:3471–3486.
Luxton GW, Gundersen GG. 2011. Orientation and function of the nuclear-centrosomal axis during cell migration. Curr Opin Cell Biol 23:579–588.
Mahaffey JP, Grego-Bessa J, Liem KF, Jr., Anderson KV. 2013. Cofilin and Vangl2 cooperate in the initiation of planar cell polarity in the mouse embryo. Development 140:1262–1271.
Marlow F, Topczewski J, Sepich D, Solnica-Krezel L. 2002. Zebrafish Rho kinase 2 acts downstream of Wnt11 to mediate cell polarity and effective convergence and extension movements. Curr Biol 12:876–884.
Marlow F, Zwartkruis F, Malicki J, Neuhauss SC, Abbas L, Weaver M, Driever W, Solnica-Krezel L. 1998. Functional interactions of genes mediating convergent extension, knypek and trilobite, during the partitioning of the eye primordium in Zebrafish. Dev Biol 203:382–399.
Martin AC, Kaschube M, Wieschaus EF. 2009. Pulsed contractions of an actin-myosin network drive apical constriction. Nature 457: 495–499.
Matis M, Russler-Germain DA, Hu Q, Tomlin CJ, Axelrod JD. 2014. Microtubules provide directional information for core PCP function. Elife 3:e02893.
Mendieta-Serrano MA, Schnabel D, Lomeli H, Salas-Vidal E. 2013. Cell proliferation patterns in early Zebrafish development. Anat Rec (Hoboken) 296:759–773.
Miller PM, Folkmann AW, Maia AR, Efimova N, Efimov A, Kaverina I. 2009. Golgi-derived CLASP-dependent microtubules control Golgi organization and polarized trafficking in motile cells. Nat Cell Biol 11:1069–1080.
Mironov AA, Beznoussenko GV. 2011. Molecular mechanisms responsible for formation of Golgi ribbon. Histol Histopathol 26: 117–133.
Montcouquiol M, Sans N, Huss D, Kach J, Dickman JD, Forge A, Rachel RA, Copeland NG, Jenkins NA, Bogani D, Murdoch J, Warchol ME, Wenthold RJ, Kelley MW. 2006. Asymmetric localization of Vangl2 and Fz3 indicate novel mechanisms for planar cell polarity in mammals. J Neurosci 26:5265–5275.
Nagele RG, Hunter E, Bush K, Lee HY. 1987. Studies on the mechanisms of neurulation in the chick: morphometric analysis of force distribution within the neuroepithelium during neural tube formation. J Exp Zool 244:425–436.
Nakamura N, Rabouille C, Watson R, Nilsson T, Hui N, Slusarewicz P, Kreis TE, Warren G. 1995. Characterization of a cis-Golgi matrix protein, GM130. J Cell Biol 131:1715–1726.
Nakaya Y, Sheng G. 2013. EMT in developmental morphogenesis. Cancer Lett 341:9–15.
Nelson WJ. 2009. Remodeling epithelial cell organization: transitions between front-rear and apical-basal polarity. Cold Spring Harb Perspect Biol 1:a000513.
Newman-Smith E, Kourakis MJ, Reeves W, Veeman M, Smith WC. 2015. Reciprocal and dynamic polarization of planar cell polarity core components and myosin. Elife 4.
Nieto MA. 2013. Epithelial plasticity: a common theme in embryonic and cancer cells. Science 342:1234850.
Nilsson T, Pypaert M, Hoe MH, Slusarewicz P, Berger EG, Warren G. 1993. Overlapping distribution of two glycosyltransferases in the Golgi apparatus of HeLa cells. J Cell Biol 120:5–13.
Ossipova O, Kim K, Sokol SY. 2015. Planar polarization of Vangl2 in the vertebrate neural plate is controlled by Wnt and Myosin II signaling. Biol Open 4:722–730.
Park EC, Cho GS, Kim GH, Choi SC, Han JK. 2011. The involvement of Eph-Ephrin signaling in tissue separation and convergence during Xenopus gastrulation movements. Dev Biol 350: 441–450.
Piel M, Meyer P, Khodjakov A, Rieder CL, Bornens M. 2000. The respective contributions of the mother and daughter centrioles to centrosome activity and behavior in vertebrate cells. J Cell Biol 149:317–330.
Quesada-Hernandez E, Caneparo L, Schneider S, Winkler S, Liebling M, Fraser SE, Heisenberg CP. 2010. Stereotypical cell division orientation controls neural rod midline formation in Zebrafish. Curr Biol 20:1966–1972.
Rabouille C, Kondylis V. 2007. Golgi ribbon unlinking: an organelle-based G2/M checkpoint. Cell Cycle 6:2723–2729.
Revenu C, Gilmour D. 2009. EMT 2.0: shaping epithelia through collective migration. Curr Opin Genet Dev 19:338–342.
Revenu C, Streichan S, Dona E, Lecaudey V, Hufnagel L, Gilmour D. 2014. Quantitative cell polarity imaging defines leader-to-follower transitions during collective migration and the key role of microtubule-dependent adherens junction formation. Development 141:1282–1291.
Rios RM. 2014. The centrosome-Golgi apparatus nexus. Philos Trans R Soc Lond B Biol Sci 369.
Ripoche J, Link B, Yucel JK, Tokuyasu K, Malhotra V. 1994. Location of Golgi membranes with reference to dividing nuclei in syncytial Drosophila embryos. Proc Natl Acad Sci U S A 91: 1878–1882.
Rodriguez-Boulan E, Macara IG. 2014. Organization and execution of the epithelial polarity programme. Nat Rev Mol Cell Biol 15: 225–242.
Rohani N, Parmeggiani A, Winklbauer R, Fagotto F. 2014. Variable combinations of specific ephrin ligand/Eph receptor pairs control embryonic tissue separation. PLoS Biol 12:e1001955.
Row RH, Maitre JL, Martin BL, Stockinger P, Heisenberg CP, Kimelman D. 2011. Completion of the epithelial to mesenchymal transition in Zebrafish mesoderm requires Spadetail. Dev Biol 354:102–110.
Ruprecht V, Wieser S, Callan-Jones A, Smutny M, Morita H, Sako K, Barone V, Ritsch-Marte M, Sixt M, Voituriez R, Heisenberg CP. 2015. Cortical contractility triggers a stochastic switch to fast amoeboid cell motility. Cell 160:673–685.
Sanders AA, Kaverina I. 2015. Nucleation and Dynamics of Golgi-derived Microtubules. Front Neurosci 9:431.
Schindelin J, Arganda-Carreras I, Frise E, Kaynig V, Longair M, Pietzsch T, Preibisch S, Rueden C, Saalfeld S, Schmid B, Tinevez JY, White DJ, Hartenstein V, Eliceiri K, Tomancak P, Cardona A. 2012. Fiji: an open-source platform for biological-image analysis. Nat Methods 9:676–682.
Schmoranzer J, Kreitzer G, Simon SM. 2003. Migrating fibroblasts perform polarized, microtubule-dependent exocytosis towards the leading edge. J Cell Sci 116:4513–4519.
Sepich DS, Usmani M, Pawlicki S, Solnica-Krezel L. 2011. Wnt/PCP signaling controls intracellular position of MTOCs during gastrulation convergence and extension movements. Development 138:543–552.
Shimada Y, Yonemura S, Ohkura H, Strutt D, Uemura T. 2006. Polarized transport of Frizzled along the planar microtubule arrays in Drosophila wing epithelium. Dev Cell 10:209–222.
Shindo A, Wallingford JB. 2014. PCP and septins compartmentalize cortical actomyosin to direct collective cell movement. Science 343:649–652.
Singh S, Solecki DJ. 2015. Polarity transitions during neurogenesis and germinal zone exit in the developing central nervous system. Front Cell Neurosci 9:62.
Slanchev K, Carney TJ, Stemmler MP, Koschorz B, Amsterdam A, Schwarz H, Hammerschmidt M. 2009. The epithelial cell adhesion molecule EpCAM is required for epithelial morphogenesis and integrity during Zebrafish epiboly and skin development. PLoS Genet 5:e1000563.
Solnica-Krezel L. 2005. Conserved patterns of cell movements during vertebrate gastrulation. Curr Biol 15:R213–228.
Solnica-Krezel L, Stemple DL, Mountcastle-Shah E, Rangini Z, Neuhauss SC, Malicki J, Schier AF, Stainier DY, Zwartkruis F, Abdelilah S, Driever W. 1996. Mutations affecting cell fates and cellular rearrangements during gastrulation in Zebrafish. Development 123:67–80.
Song H, Hu J, Chen W, Elliott G, Andre P, Gao B, Yang Y. 2010. Planar cell polarity breaks bilateral symmetry by controlling ciliary positioning. Nature 466:378–382.
Stevenson BR, Siliciano JD, Mooseker MS, Goodenough DA. 1986. Identification of ZO-1: a high molecular weight polypeptide associated with the tight junction (zonula occludens) in a variety of epithelia. J Cell Biol 103:755–766.
Sumanas S, Kim HJ, Hermanson SB, Ekker SC. 2002. Lateral line, nervous system, and maternal expression of Frizzled 7a during Zebrafish embryogenesis. Mech Dev 115:107–111.

Sutterlin C, Colanzi A. 2010. The Golgi and the centrosome: building a functional partnership. J Cell Biol 188:621–628.
Tada M, Kai M. 2012. Planar cell polarity in coordinated and directed movements. Curr Top Dev Biol 101:77–110.
Takeichi M. 2014. Dynamic contacts: rearranging adherens junctions to drive epithelial remodelling. Nat Rev Mol Cell Biol 15: 397–410.
Terasaki M. 2000. Dynamics of the endoplasmic reticulum and golgi apparatus during early sea urchin development. Mol Biol Cell 11:897–914.
Thisse C, and Thisse, B.. 2005. High Throughput Expression Analysis of ZF-Models Consortium Clones. . In. ZFIN Direct Data Submission (http://zfin.org). .
Thyberg J, Moskalewski S. 1999. Role of microtubules in the organization of the Golgi complex. Exp Cell Res 246:263–279.
Tian J, Yam C, Balasundaram G, Wang H, Gore A, Sampath K. 2003. A temperature-sensitive mutation in the nodal-related gene cyclops reveals that the floor plate is induced during gastrulation in Zebrafish. Development 130:3331–3342.
Topczewski J, Sepich DS, Myers DC, Walker C, Amores A, Lele Z, Hammerschmidt M, Postlethwait J, Solnica-Krezel L. 2001. The Zebrafish glypican knypek controls cell polarity during gastrulation movements of convergent extension. Dev Cell 1:251–264.
Vinogradova T, Paul R, Grimaldi AD, Loncarek J, Miller PM, Yampolsky D, Magidson V, Khodjakov A, Mogilner A, Kaverina I. 2012. Concerted effort of centrosomal and Golgi-derived microtubules is required for proper Golgi complex assembly but not for maintenance. Mol Biol Cell 23:820–833.
Vladar EK, Bayly RD, Sangoram AM, Scott MP, Axelrod JD. 2012. Microtubules enable the planar cell polarity of airway cilia. Curr Biol 22:2203–2212.
Wallingford JB. 2010. Planar cell polarity signaling, cilia and polarized ciliary beating. Curr Opin Cell Biol 22:597–604.
Wallingford JB. 2012. Planar cell polarity and the developmental control of cell behavior in vertebrate embryos. Annu Rev Cell Dev Biol 28:627–653.
Williams M, Yen W, Lu X, Sutherland A. 2014. Distinct apical and basolateral mechanisms drive planar cell polarity-dependent convergent extension of the mouse neural plate. Dev Cell 29:34–46.
Wu SY, Shin J, Sepich DS, Solnica-Krezel L. 2012. Chemokine GPCR signaling inhibits beta-catenin during Zebrafish axis formation. PLoS Biol 10:e1001403.
Yadav S, Linstedt AD. 2011. Golgi positioning. Cold Spring Harb Perspect Biol 3.
Yadav S, Puri S, Linstedt AD. 2009. A primary role for Golgi positioning in directed secretion, cell polarity, and wound healing. Mol Biol Cell 20:1728–1736.
Yadav S, Puthenveedu MA, Linstedt AD. 2012. Golgin160 recruits the dynein motor to position the Golgi apparatus. Dev Cell 23:153–165.
Yano H, Yamamoto-Hino M, Abe M, Kuwahara R, Haraguchi S, Kusaka I, Awano W, Kinoshita-Toyoda A, Toyoda H, Goto S. 2005. Distinct functional units of the Golgi complex in Drosophila cells. Proc Natl Acad Sci U S A 102:13467–13472.
Yin C, Kiskowski M, Pouille PA, Farge E, Solnica-Krezel L. 2008. Cooperation of polarized cell intercalations drives convergence and extension of presomitic mesoderm during Zebrafish gastrulation. J Cell Biol 180:221–232.
Yin C, Solnica-Krezel L. 2007. Convergence and extension movements affect dynamic notochord-somite interactions essential for Zebrafish slow muscle morphogenesis. Dev Dyn 236:2742–2756.
Zallen JA. 2007. Planar polarity and tissue morphogenesis. Cell 129:1051–1063.
Zhang J, Webb SE, Ma LH, Chan CM, Miller AL. 2011. Necessary role for intracellular Ca2+ transients in initiating the apical-basolateral thinning of enveloping layer cells during the early blastula period of Zebrafish development. Dev Growth Differ 53:679–696.